Power Grid Sensitivity Analysis of Geomagnetically Induced Currents

Thomas J. Overbye, *Fellow, IEEE*, Komal S. Shetye, *Member, IEEE*, Trevor R. Hutchins, *Student Member, IEEE*, Qun Qiu, *Senior Member, IEEE*, and James D. Weber, *Member, IEEE*

Abstract—Geomagnetically induced currents (GICs) have the potential to severely disrupt power grid operations, and hence their impact needs to be assessed through planning studies. This paper presents a methodology for determining the sensitivity of the GICs calculated for individual and/or groups of transformers to the assumed quasi-dc electric fields on the transmission lines that induce the GICs. Example calculations are provided for two small systems and for the North American Eastern Interconnect model. Results indicate that transformer GICs are mostly due to the electric fields on nearby transmission lines, implying localized electric field models may be appropriate for such studies.

Index Terms—Geomagnetic disturbance (GMD), geomagnetically induced currents (GICs), power flow, power system sensitivity analysis.

I. INTRODUCTION

I T is now widely recognized that geomagnetic disturbances (GMDs) caused by solar activity have the potential to severely impact the operation of interconnected electric power systems worldwide. As noted in [1], the potential for GMDs to interfere with power grid operation has been known since at least the early 1940s. The basic mechanism for this interference is GMDs cause variations in the earth's magnetic field. These changes induce quasi-dc electric fields (usually with frequencies much below 1 Hz) in the earth with the magnitude and direction of the field GMD event dependent. These electric fields then cause geomagnetically induced currents (GICs) to flow in the earth's crust (with depths to hundreds of kms), and in other conductors such as the high voltage electric transmission grid. In the high voltage transformers the quasi-dc GICs produce an offset on the regular ac current that can lead to half-cycle saturation, resulting in increased transformer heating and reactive power losses [1].

The North American Electric Reliability Corporation (NERC) in a February 2012 special reliability assessment report on GMDs [2] notes that there are two primary risks associated with GICs in the bulk electric system. The first is the potential for damage to transmission system assets, primarily the high voltage transformers. The second is the loss of reactive power support leading to the potential for a voltage collapse.

This paper focuses on the second risk, building on the existing literature considering the power flow modeling needed to provide an assessment of the GIC related voltage stability risks. The paper's particular emphasis is to provide theory and case study results on the sensitivity of the transformer GICs to the assumed GMD induced electric fields.

The paper presents an approach to help power engineers determine the appropriate amount of an interconnected electric transmission system that needs to be represented in detail to correctly determine the GICs in transformers of interest. The GICs that flow in a transmission system are ultimately driven by the GMD-induced geoelectric fields at the earth's surface, with a number of papers providing details on the calculation of these fields, for example [3]–[5]. The geoelectric field calculations can be quite involved, potentially requiring detailed models of the earth's crust conductivity, and as noted in [4], [6], and [7] can be significantly influenced by the nearby presence of salt water.

However, which electric fields need to be modeled in detail is driven in part by the conductivity structure of the electric transmission system. Earlier work has shown that GICs in general do not flow over large distances in interconnected power grids [8], with [9] and [10] providing results for the Finnish 400-kV grid. This paper builds on such earlier works by providing a computationally efficient algorithm to quantify the sensitivity of the transformer GICs to the GMD induced electric fields, presenting case study results for two small systems and for a large system model of the North American Eastern Interconnect (EI).

The paper is arranged as follows. Section II describes the GIC power flow methodology, introduces a small four-bus example model and explains the need for the sensitivity analysis presented in this paper. Section III presents the sensitivity analysis algorithm while Section IV applies the algorithm to a four-bus system and the twenty bus GIC test system of [16], while Section V provides example results for a 62 500-bus model of the EI.

II. GIC POWER FLOW MODELING METHODOLOGY

The inclusion of the impact of GICs in the power flow was first described in [11] with later consideration for large

system studies in [12] and [13]. An analysis of a large scale power system such as Dominion Virginia Power was recently presented in [14].

The approach from [13] can be summarized as follows. Consider a standard m bus power flow model (e.g., positive sequence) in which the m buses are grouped into s substations; let n = m + s. Because the GICs are considered to be dc, how they flow through the power grid can be determined by solving

$$\mathbf{V} = \mathbf{G}^{-1}\mathbf{I} \tag{1}$$

where $\mathbf{G}$ is an n by n symmetric matrix similar in form to the power system bus admittance matrix, except 1) it is a real matrix with just conductance values, 2) the conductance values are determined by the parallel combination of the three individual phase resistances, 3) $\mathbf{G}$ is augmented to include the substation neutral buses and substation grounding resistance values, 4) transmission lines with series capacitive compensation are omitted since series capacitors block dc flow, and 5) the transformers are modeled with their winding resistance to the substation neutral and in the case of autotransformers both the series and common windings are represented. Of course for large systems $\mathbf{G}$ is quite sparse and hence (1) can be solved with computational effort equivalent to a single power flow iteration. When solved the voltage vector $\mathbf{V}$ contains entries for the s substation neutral dc voltages and the m bus dc voltages.

The vector $\mathbf{I}$ models the impact of the GMD-induced electric fields as Norton equivalent dc current injections. Two main methods have been proposed for representing this electric field variation in the power grid: either as dc voltage sources in the ground in series with the substation grounding resistance or as dc voltage sources in series with the transmission line resistances [11], [15]. In both approaches these Thevenin equivalent voltages are converted to Norton equivalent currents that are then used in $\mathbf{I}$. In [15] it was shown that while the two methods are equivalent for uniform electric fields, only the transmission line approach can handle the non-uniform electric fields that would be expected in a real GMD event. This is the approach used in this paper.

Using the approach of [15], to calculate the GMD-induced voltage on transmission line k, U_k, the electric field is just integrated over the length of the transmission line [16]

$$U_k = \int_R \bar{E} \cdot d\bar{l} \tag{2}$$

where R is the geographic route of transmission line k, $\bar{E}$ is the electric field along this route, and $d\bar{l}$ is the incremental line segment. Note, here we use the symbol U for the voltages induced in the lines to differentiate from the bus and substation voltages in (1).

If the electric field is assumed to be uniform over the route of the transmission line then (2) is path independent and can be solved by just knowing the geographic location of the transmission line's terminal buses. In this case (2) can be simplified to either

$$U_k = E_{k,N}L_{k,N} + E_{k,E}L_{k,E} \tag{3}$$

when expressed in rectangular coordinates, or

$$U_k = E_k\, L_k \cos(\theta_{k,E} - \theta_{k,L}) \tag{4}$$

if polar coordinates are used. In (3) $E_{k,N}$ is the northward electric field (V/km) over line k, $E_{k,E}$ is the eastward electric field (V/km), $L_{k,N}$ is the line's northward distance (km), and L_E is the eastward distance (km). In (4) E_k is the magnitude of the electric field (V/km), $\theta_{k,E}$ is its compass direction (with north defined as 0 degrees), L_k is the distance between the two terminal substations of the line, and $\theta_{k,L}$ is the compass direction from the substation of the arbitrarily defined "from" bus i to the substation of the "to" bus j.

Define the electric field tangential to the line as

$$E_{k,T} = E_k\,\cos(\theta_{k,E} - \theta_{k,L}). \tag{5}$$

Then using (5), (4) simplifies to

$$U_k = E_{k,T}L_k. \tag{6}$$

The degree of solution error introduced by assuming a uniform field over a line's route is one of the contributions of this paper. However, it is important to note that assuming the electric field is uniform over the path of a particular line is quite different than assuming the field is uniform throughout the study footprint. Because GMDs are continental in scope, the variation in the electric field over most line lengths would likely not be significant. In the case of long lines, the voltage can be approximated by dividing the line into segments, and assuming a uniform field over the individual segments, and then summing the results.

In developing the sensitivity analysis in the next section, it is useful to modify (1) to write the input in terms of the vector of electric field magnitudes tangential to each of the K transmission lines in the system

$$\mathbf{V} = \mathbf{G}^{-1}\mathbf{B}\mathbf{E}_T \tag{7}$$

where $\mathbf{E}_T$ is a K-dimensional real vector with entries giving the magnitude of the electric field tangential to each line, as per (5). $\mathbf{B}$ is an n by K real matrix in which each column, corresponding to line k, has non-zeros only at the location of the "from" end bus i and the "to" end bus j; the magnitude of these values is the line's conductance, g_k, multiplied by the distance between the line's terminal, L_k, with a sign convention such that the "from" end has a positive value, and the "to" end a negative value.

Before moving on to the sensitivity derivation, it may be helpful to introduce a small example system. Consider the three substation (s = 3), four-bus (m = 4) system shown in Fig. 1 with Bus 1 in Substation A, Buses 2 and 3 in Substation B and Bus 4 in Substation C. Assume all the substations have grounding resistance 0.2 Ω, that the Bus 1 generator has an implicitly modeled generator step-up (GSU) transformer with resistance of 0.15 Ω/phase on the high (wye-grounded) side (0.05 Ω for the three phases in parallel), and that the Bus 4 generator has a similar GSU transformer with 0.15 Ω/phase. There is a 345-kV transmission line between Buses 1 and 2 with resistance of 3 Ω/phase, and a 500-kV line between Buses 3

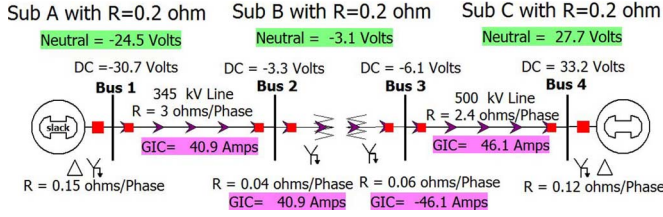Fig. 1.   Three substation, four-bus GIC example.

TABLE I
G MATRIX (IN SIEMENS) FOR THE FOUR-BUS SYSTEM

	SubA	SubB	SubC	1	2	3	4
SubA	25	0	0	-20	0	0	0
SubB	0	80	0	0	-75	0	0
SubC	0	0	30	0	0	0	-25
1	-20	0	0	21	-1	0	0
2	0	-75	0	-1	126	-50	0
3	0	0	0	0	-50	51.25	-1.25
4	0	0	-25	0	0	-1.25	26.25

TABLE II
B$^\mathrm{T}$ MATRIX (IN SIEMENS-KM) FOR THE FOUR-BUS SYSTEM

Line ↓	SubA	SubB	SubC	1	2	3	4
1 to 2	0	0	0	150	-150	0	0
3 to 4	0	0	0	0	0	187.5	-187.5

TABLE III
V$^\mathrm{T}$ VECTOR (IN VOLTS) FOR THE FOUR-BUS SYSTEM

	SubA	SubB	SubC	1	2	3	4
Voltage	-24.5	-3.1	27.7	-30.7	-3.3	-6.1	33.2

and 4 with a resistance of 2.4 Ω/phase. Buses 2 and 3 are connected through a wye-grounded autotransformer with resistance of 0.04 Ω/phase for the common winding and 0.06 Ω/phase for the series winding.[1]

Assume the substations are at the same latitude, with Substation A 150 km to the west of B, and C 150 km to the east of B. With a 1 V/km assumed eastward GMD induced electric field (parallel to the lines), (6) gives induced voltages of 150 V for each of the lines. The system **G** matrix is shown in Table I and the **B** matrix in Table II. With an assumed eastward electric field of 1 V/km the input vector is

$$\mathbf{E}_\mathrm{T} = \begin{bmatrix} 1.0 \\ 1.0 \end{bmatrix}. \tag{8}$$

Substituting this into (7) gives the voltage vector **V** values shown in Table III.

Once the voltages are known, the GICs flowing in the transmission lines and transformers can be determined by just solving the dc circuit equation for each line, including the GMD induced series voltage for each of the transmissions lines. A potential point of confusion in interpreting the results

[1]Since the concept of per unit plays no role in GIC determination, resistance values are expressed in Ohms (Ω), current is in amps (A), and the dc voltages are given in volts (V).

of the GIC calculations is to differentiate between the per phase GICs in transmission lines and transformers, and the total three phase GICs in these devices. Since the three phases are in parallel, the conversion between the two is straightforward with the total current just three times the per phase current. The convention commonly used for GIC analysis is to use the per phase current for transformers and transmission lines, and the total three phase current for the substation neutral current. Thus for the Fig. 1 system the current flowing in the transmission line between Buses 1 and 2 is

$$\frac{E_{21} + V_1 - V_2 +}{3\ \Omega/\text{phase}} = \frac{(150 - 30.67 + 3.34)}{3} = 40.9\ \text{A/phase}. \tag{9}$$

The coupling between the GIC calculations and the power flow is the GIC-induced reactive power loss for each transformer r, which is usually modeled as a linear function of the effective GIC through the transformer [1], [17], [18] with [19] making the observation that these reactive power losses vary linearly with terminal voltage

$$Q_{GIC,r} = V_{pu,r} K_r I_{Effective,r} \tag{10}$$

where $Q_{GIC,r}$ is the additional reactive power loss for the transformer (in Mvar), $V_{pu,r}$ is the per unit ac terminal voltage for the transformer, and K_r is a transformer specific scalar with units Mvars/amp.

The value of $I_{Effective,r}$ used in (10) is an "effective" per phase value that depends on the type of transformer. In the simplest case of a grounded wye-delta, such as is common for GSU transformers, $I_{Effective,r}$ is straightforward—just the current in the grounded (high-side) winding. For transformers with multiple grounded windings and autotransformers the value of $I_{Effective,r}$ depends upon the current in both coils [11]. Here we use the approach of [18] and [13]

$$I_{Effective,r} = |I_{GICH,r} + \frac{I_{GICL,r}}{a_{t,r}}| \tag{11}$$

where $I_{GICH,r}$ is the per phase GIC going into the high side winding (i.e., the series winding of an autotransformer), $I_{GICL,r}$ is the per phase GIC going into the low side of the transformer, and $a_{t,r}$ is the standard transformer turns ratio (high voltage divided by low voltage). Note, for an autotransformer the current going into the common winding would just be

$$I_{GIC,Common,r} = I_{GICH,r} + I_{GICL,r}. \tag{12}$$

The last step needed to facilitate the derivation of the transformer effective current sensitivities is to define a column vector $\mathbf{C}_r$ of dimension n such that

$$I_{Effective,r} = |\mathbf{C}_r \mathbf{V}| = |\mathbf{C}_r \mathbf{G}^{-1} \mathbf{B}\ \mathbf{E}_T| \tag{13}$$

where $\mathbf{C}_r$ is quite sparse, containing the per phase conductance values relating the GIC bus and substation dc voltages to the current. For a GSU transformer with a single grounded coil going between bus i and substation neutral s with conductance g_{is}, the only nonzeros in $\mathbf{C}_r$ would be g_{is} at the bus i position, and $-g_{is}$ at

TABLE IV
$\mathbf{C}$ Vectors (in Siemens) for the four-bus System;
Note Values Are Conductance Per Phase as Opposed
to the Three Phase Values Used in $\mathbf{G}$

Transformer $\downarrow$	SubA	SubB	SubC	1	2	3	4
Bus 1 GSU	-6.7	0	0	6.7	0	0	0
Bus 4 GSU	0	0	-8.3	0	0	0	8.3
Bus 2-3	0	-17.25	0	0	12.1	5.2	0

the substation neutral s position. For an autotransformer between series bus i, common bus j and substation neutral s, (11) is

$$
\begin{aligned}
I_{Effective,r} &= \left| (V_i - V_j)g_{ij} + \frac{(V_j - V_s)g_{js} - (V_i - V_j)g_{ij}}{a_{t,r}} \right| \\
&= \left| V_i \left(g_{ij} - \frac{g_{ij}}{a_{t,r}} \right) + V_j \left(\left(\frac{g_{js} + g_{ij}}{a_{t,r}} \right) - g_{ij} \right) \right. \\
&\quad \left. - \left(\frac{V_s g_{js}}{a_{t,r}} \right) \right|.
\end{aligned}
\tag{14}
$$

The $\mathbf{C}$ vectors for the three transformers in the four-bus example are given in Table IV. Using these values and $\mathbf{V}$ from Table III the $I_{\text{effective}}$ values of 40.9 amps (Bus 1 GSU), 46.1 amps (Bus 4 GSU) and 17.9 amps (Bus 2 to 3 Autotransformer) are readily verified.

III. Sensitivity Analysis

A key concern in performing a power flow GIC impact study is to know the sensitivity of the results to the input electric field assumptions. Motivated by the optimal power flow control sensitivities in [20], differentiating (13) with respect to the electric field vector input gives a column vector of dimension K

$$
\frac{dI_{\text{Effective,r}}}{d\mathbf{E}_T} = \pm \mathbf{C}_r \, \mathbf{G}^{-1} \mathbf{B} = \pm \mathbf{S}_{T,r}
\tag{15}
$$

with the $\pm$ resolved using the sign of the absolute value argument from (13). The interpretation of these results is each entry k in $\mathbf{S}_{T,r}$, $\mathbf{S}_{T,r}[k]$, tells how $I_{\text{Effective}}$ for the rth transformer would vary for a 1 V/km variation in the electric field tangential to the path of transmission line k.

Then from (13) and (15), and referring back to the direction definitions from (4)

$$
\begin{aligned}
I_{\text{Effective,r}} &= |\mathbf{C}_r \mathbf{G}^{-1} \mathbf{B} \mathbf{E}_T| = |\mathbf{S}_{T,r} \mathbf{E}_T| \\
&= \left| \sum_{k=1}^{K} (\mathbf{S}_{T,r}[k] \, \mathbf{E}_T[k]) \right| \\
&= \sum_{k=1}^{K} (\mathbf{S}_{T,r}[k] \, \mathbf{E}[k] \cos(\theta_{k,E} - \theta_{k,L}))
\end{aligned}
\tag{16}
$$

in which the elements of the summation indicate the contribution to $I_{\text{Effective}}$ for the rth transformer provided by each line in the system for the case of a (potentially) non-uniform field. In the case of a uniform field applied to the entire case then $\theta_{k,E}$ will be the same for all the transmission lines.

Several observations are warranted. First, from a computational perspective (15) is quite straightforward to evaluate. Since $\mathbf{G}$ is symmetric, once it has been factored $\mathbf{C}_r \mathbf{G}^{-1}$ can be solved with just a forward and backward substitution.

Furthermore, since $\mathbf{C}_r$ is quite sparse, sparse vector methods [21] could be used to quickly perform at least the forward substitution, and the backward substitution if results are only needed for a limited portion of the system.

Second, the magnitude of the entries in $\mathbf{S}_r$ indicate the transmission lines that are most important in contributing to $I_{\text{Effective,r}}$ for a uniform field, with the simple scaling from (16) generalizing to the non-uniform case. Hence a more accurate knowledge of the electric field associated with the most sensitive lines is warranted, and as will be shown in large cases, often most of the lines have little influence and hence information about their electric fields is irrelevant.

Third, since during a particular GMD the field direction could change rapidly, and certainly may not be the same everywhere, the L1-norm of $\mathbf{S}_{T,r}$ actually provides the worst case scenario for a uniform electric field storm. That is, the sum of the absolute values of the elements of $\mathbf{S}_{T,r}$ tell the absolute maximum value for $I_{\text{Effective,r}}$ in the unlikely event that a 1 V/km storm was oriented tangentially to all the transmission lines. Or, perhaps more usefully, tangential to the lines most important to transformer r.

Fourth, the previous observation can be generalized for the non-uniform case by defining

$$
I_{\max,r} = \sum_{k=1}^{K} (|\mathbf{S}_{T,r}[k]| |\mathbf{E}[k]|)
\tag{17}
$$

where each of the elements in the summation tells the maximum GIC current that could be contributed by each transmission line when subjected to the specified non-uniform field aligned tangentially to the line.

Fifth, one of the issues associated with GMD assessment is the observation that the GICs are often lower for those transformers located in the "interior" of the network compared to those located on the "edge" since for the interior transformers the GICs flowing into one side of the transformer's substation tend to be canceled by those flowing out the other side [22], [18], [23], [24]. This is not the case for those on the edge, defined as a location in which most of the transmission lines leave the substation in a similar direction. Edges are often caused by geographic constraints such as water or mountains, or by more arbitrary ones such as utility service territory boundaries in which transmission lines emanate from generators near the boundary in a common direction. Here we propose a measure to quantify this effect

$$
\Lambda_r = \frac{I_{\text{Effective,r}}}{I_{\max,r}}
\tag{18}
$$

with the value of $I_{\max,r}$, which is calculated using (17), dependent on an assumed direction for the field. However Λ_r is independent of the magnitude of $\mathbf{E}$ since its values are used in both the numerator and denominator. Higher values of Λ_r indicate transformers closer to a network edge.

Finally, this analysis can easily be extended to allow consideration of multiple transformers simultaneously. For example, one may be interested in knowing the sensitivity of the sum of the effective currents for all the transformers in a particular set R. This can be done by defining

$$
\mathbf{C} = \sum_{r=1}^{R} (\pm \mathbf{C}_r)
\tag{19}
$$

TABLE V
TRANSPOSE OF $\mathbf{S_T}$ VECTORS FOR THE FOUR-BUS SYSTEM

Transmission Lines↓	Bus 1 GSU	Bus 4 GSU	Bus 2-3 Auto
Line 1 -- 2	35.02	5.87	-18.30
Line 3 -- 4	5.87	40.25	36.21

again with the $\pm$ resolved using the sign of the absolute value argument from (13) for each transformer r. Then

$$\frac{dI_{\text{Effective}}}{d\mathbf{E}_T} = \mathbf{C}\,\mathbf{G}^{-1}\mathbf{B} = \mathbf{S}_T \qquad (20)$$

tells the dependence of the effective currents for all the transformers in set R on the electric fields for each of the transmission lines. Hence the incremental impact on $I_{\text{Effective}}$ to a change in any (or all) of the assumed electric fields can be readily calculated. Also, if desired the sensitivity of the total GIC related reactive power losses for the transformers in R could be determined by scaling the values in each $\mathbf{C}_r$ by the coefficients from (10).

The next section provides examples of these sensitivity calculations using the earlier four-bus system along with the 20 bus example from [16]. Then, the following section provides some results from the 62 500-bus EI model with a focus on the American Electric Power (AEP) East footprint.

IV. SMALL SYSTEM EXAMPLES

For the four-bus system introduced previously with the assumed eastward electric field of 1 V/km, using (15) gives the sensitivity values shown in Table V. As noted immediately following (15), since the transformer effective currents are defined using an absolute value, the sign of the associated sensitivities depends upon whether the argument in the absolute value function of (13) is positive or negative. For the four-bus system the values are positive for the Bus 1 GSU and the autotransformer, and negative for the Bus 4 GSU, resulting in a change in sign for the Bus 4 GSU values shown in Table V. Since the electric field is 1 V/km and applied tangentially to each line, the $I_{\text{Effective}}$ for each transformer can be verified using (16) as just the sum of values in each column.

The strong dependence of the transformer effective currents on the nearby lines is immediately apparent in Table V. For example, the Bus 1 GSU $I_{\text{Effective}}$ is more than six times as sensitive to the electric field on the adjacent line between Buses 1 and 2, compared with the more distant line between Buses 3 and 4. The cancellation effect is also apparent for the interior autotransformer compared to the two edge GSUs, with the electric field on the line between Buses 1 and 2 actually helping to decrease the effective current for the autotransformer. In this example since the two transmission lines point in the same direction, the value of Λ_r is 1.0 for each of the GSUs. For the autotransformer (17) indicates the "worst case" scenario for a 1 V/km field would be if it were oriented east to west on one side of the transformer, and west to east on the other side, funneling all of the GICs into the autotransformer. The value of Λ_r is

$$\Lambda_{2-3} = \frac{(36.21 - 18.30)}{(36.21 + 18.30)} = 0.329 \qquad (21)$$

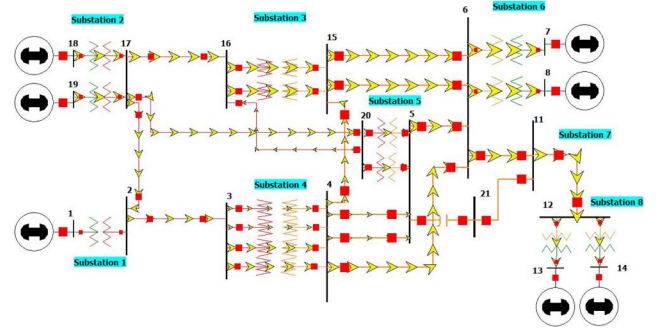with the lower value indicating an interior location.

Fig. 2. Twenty-bus GIC test system one-line showing 1 V/km eastward values.

TABLE VI
TRANSPOSE OF $\mathbf{S_T}$ VECTORS FOR TWO
TRANSFORMERS FROM THE TWENTY-BUS SYSTEM

	T3, 18-17 Eastward	T3, 18-17 Max	T8, 20-5 Eastward	T8, 20-5 Max
$I_{\text{effective}}$	31.55	48.09	13.07	92.1
Line 2-3	5.82	5.84	-2.53	2.53
Line 17-2	-4.50	5.84	1.95	2.54
Line 15-4	0.62	0.65	8.07	8.55
Line 17-16	11.64	12.01	-0.79	0.82
Line 4-5,1	1.35	1.65	-11.38	13.95
Line 4-5,2	1.35	1.65	-11.38	13.95
Line 5-6	0.76	0.81	21.57	23.16
Line 5-11	0.00	0.00	0.00	0.00
Line 6-11	-0.05	0.25	-0.25	1.23
Line 4-6	2.46	2.47	9.19	9.21
Line 15-6,1	1.72	1.81	0.63	0.66
Line 15-6,2	1.72	1.81	0.63	0.66
Line 11-12	0.40	0.40	1.98	1.98
Line 16-20	0.01	0.46	-0.06	6.03
Line 17-20	8.27	12.45	-4.55	6.86

Next the algorithm is applied to the twenty bus test system from [16]. A one-line of the system is shown in Fig. 2, in which the arrows visualize the flow of the GICs for the 1 V/km eastward (90 degree) field scenario; the size of the arrow is proportional to the GICs on each of the devices.

Table VI gives the sensitivity values for two transformers, GSU Transformer T3 going between Buses 18 and 17 (shown on the upper left edge of the one-line) and autotransformer T8 going between Buses 20 and 5 (shown in the middle of the one-line). For the 1 V/km eastward field the effective currents are 31.55 A for T3 and 13.07 A for T8 with the amounts contributed by each line given in columns two and four, respectively. Columns three and five give the line contributions assuming a tangential field. For this field direction the values of the Λ's are

$$\Lambda_{T3} = \frac{31.55}{48.09} = 0.656$$

$$\Lambda_{T8} = \frac{13.07}{92.10} = 0.142 \qquad (22)$$

indicating, respectively, their edge and interior locations.

As was the case for the four-bus system, for T3 large amount of the GICs are contributed by the nearby transmission lines with the three first neighbor transmission lines (i.e., those directly connected to the transformer), (2-17, 17-16, 17-20), contributing $(-4.50 + 11.64 + 8.27) = 15.41$ A (48.8%), while the second neighbor lines (2-3, 16-20) contribute another 18.5%;

TABLE VII
SENSITIVITY ANALYSIS OF CERTAIN TRANSFORMERS IN THE AEP EAST AREA

| Transformer Name, Nominal KV and Type	A, 765/345 kV Autotransformer (e)	B, 765/26 kV GSU (e)	C, 765/345 kV Autotransformer (e)	D, 345/138 kV Autotransformer (m)	E, 765/345 kV Autotransformer (m)	F, 345/138 kV Autotransformer (m)
$I_{max,r}$	22.106	69.739	82.917	33.473	157.461	66.755
Highest % contribution to $I_{max,r}$ by a line	37.904	33.026	46.097	10.815	20.866	17.031
No. of lines contributing to 75% of $I_{max,r}$	10 (total) 4 (connecting 1st neighbor buses)	5 (all are connected to 1st neighbor buses)	16 (total) 9 (connecting 1st neighbor buses)	24 (total) 9 (connecting 1st neighbor buses)	9 (all are connected to 1st neighbor buses)	25 (total) 12 (connecting 1st neighbor buses)
Proximity of the 75% contributing lines	23 – 280 km	45 - 234 km	5 – 190 km	9 – 234 km	31 – 280 km	6 – 151 km
No. of lines contributing to 90% of $I_{max,r}$	39	22	90	90	46	87
$I_{Effective,r}$ for a 0 degree, 1 V/km electric field ($I_{Effective,r}0$)	10.526	38.194	32.011	5.359	32.105	11.301
$\Lambda_{r0} = I_{Effective,r}0 / I_{max,r}$	0.476	0.548	0.386	0.16	0.204	0.169
$I_{Effective,r}$ for a 90 degree, 1 V/km electric field ($I_{Effective,r}90$)	2.352	17.344	20.461	1.719	29.298	7.742
$\Lambda_{r90} = I_{Effective,r}90 / I_{max,r}$	0.106	0.249	0.247	0.051	0.186	0.116
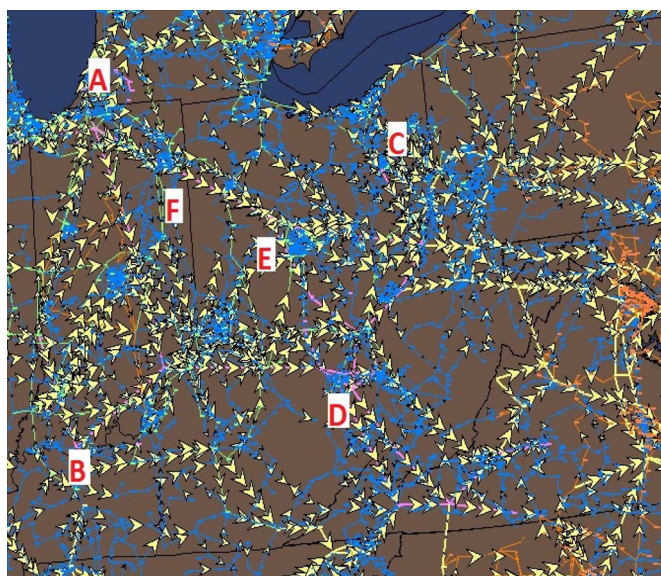
Fig. 3. Portion of EI encompassing the AEP East system footprint with GIC flows and Table VII transformer locations.

the most distant lines (6-11, 11-20) contribute only about 1%. This effect is less dramatic for T8 because of 1) the relatively small system size, and 2) its more central location. In the next section the dependence of the effective currents on the more local transmission lines will be demonstrated using the much larger EI model.

V. LARGE CASE EXAMPLES

In this section sensitivity analysis is demonstrated using a 62 500-bus, 7500-transformer, 57 500-transmission line EI model. Here the analysis is focused on a subsystem of the EI model, the American Electric Power (AEP) East footprint that covers a portion of the eastern US shown in Fig. 3. In the model AEP East contains about 1300 buses, 275 transformers, and

1900 transmission lines. The figure uses yellow arrows to show the magnitude and direction of the GIC flows for an assumed 1 V/km uniform eastward field applied to the entire EI.

Table VII shows the results of the sensitivity analysis, with the transformers at the edges of the network marked as (e), and the ones in the middle of the system marked as (m). The location of the six Table VII transformers, arbitrarily named A–F, are indicated on the figure. Some of these transformers were selected based on the results of a previous study [24], wherein the transformers that are likely to exhibit the highest neutral currents for various electric field scenarios were determined.

Several key transformers, including GSUs and auto-transformers, of different nominal voltages and locations were investigated. For each transformer the table shows 1) the value $I_{max,r}$, computed using (17), 2) some statistics on the transmissions lines that contributed to this value calculated using (15), and 3) the values of $I_{Effective,r}$ and Λr computed using an assumed northward (0 degree) and an assumed eastward (90 degree) uniform 1 V/km electric field.

Table VII indicates that for these transformers, GICs are localized, in that out of the 57 500 transmission lines in the entire study footprint, less than 100 lines account for 90% of the GIC in a particular transformer. This means that while performing a GMD analysis, accurate information of the GMD induced voltages on only this small subset of transmission lines would ultimately be needed.

In the case of transformers located at the edges of the network, the most sensitive line for a particular transformer contributes a higher percentage of GICs than the most sensitive line for a transformer located in the middle of the network. The value of $I_{max,r}$ for a given transformer represents the absolute worst case maximum $I_{Effective,r}$ value for a 1 V/km electric field. Comparing this to the actual $I_{Effective,r}$ for a northward (0 degree) or an eastward (90 degree) field, the table shows that the overestimation of the effective GICs, indicated by $I_{max,r}$, over the actual effective value is higher in the cases of transformers in the middle than those at the edges.

Also the results show that the 765 kV lines contribute most of the GICs to these transformers. This can be attributed to the fact that they connect the first neighbor buses to the transformers of interest (with the term "first neighbor buses" used to indicate buses that are connected to a terminal of the transformer through a single transmission line). It also appears that the number of first neighbor buses is proportional to the number of lines necessary to contribute 75% of that transformer's GIC. The data shows that the fewer the first neighbor buses, the fewer lines required to contribute 75% of the transformers GIC.

Finally, to get a feel for the transmission lines GIC contributions for the entire AEP East footprint, (19) and (20) were used with R defined as the set of the 60 AEP East transformers with the largest effective currents. With a 1 V/km uniform eastward field the net $I_{\text{Effective}}$ for these 60 transformers is 666.3 A. Of this 629.4 A (94.4%) is contributed by AEP East transmission lines (including tie-lines), with a single 765 kV line contributing almost 10%. Overall the ten transmission lines with the highest contributions provide 52% of the total, while the highest twenty lines contribute 76% of the total effective transformer GICs. Results are similar for a northward field, with a total $I_{\text{Effective}}$ of 684.0 A with 647.9 A (94.7%) contributed by AEP East lines. In both cases about 1% of the transmission lines contributed about 99% of the GICs, and geographically these lines were relatively close to the affected transformers.

The ramification is that detailed knowledge of the GMD-induced electric fields is probably needed only for transmission lines within or nearby to the study footprint, and that this set of transmission lines can be computed with good computational efficiency using (20), which does not require a priori electric field knowledge. This is a quite useful result since in some geographic locations, such as near salt water or in locations with varying crust conductivity, the field calculations can be involved. For footprints outside such regions simpler models, perhaps even uniform electric fields, could be used. Even for footprints containing more complex geographic locations, the more detailed electric field calculations are only needed for the footprint itself and nearby locations.

VI. Summary and Future Work

This paper has presented a computationally efficient algorithm for determining the set of transmission lines that contribute most to the effective GICs in a specified set of transformers. Large system results have indicated that the detailed GMD induced electric fields are often only needed for transmission lines within or nearby to a specified study footprint.

In closing it is important to note issues that are left for future work. First, this paper has not considered the dependence of the results on the size of the system model itself. That is, the size of the $\mathbf{G}$ matrix. From a computational perspective this isn't a significant limitation since the matrix can be quickly factored even for large systems such as the EI. However, obtaining the GIC specific parameters needed to construct $\mathbf{G}$, such as the substation grounding resistance, can sometimes be difficult. As was mentioned in [13], default parameters can be used if necessary, but quantification of the associated error is an area for future research.

Second, this paper has not addressed the issue of how large of a study footprint is needed. If computational speed is a key concern, then this paper suggests the ability to first create a smaller equivalent system, with the equivalent explicitly retaining the most sensitive lines. A variety of equivalencing approaches could be used, with [25] providing a good overview of the possible methods. The size of the equivalent system would depend, in part, upon the focus of the study. As mentioned in the introduction (from [2]), there are two primary risks to the bulk grid from GICs: damage to transformers due to increased heating and loss of reactive support leading to voltage collapse. Just knowing the transformer GICs can be helpful with the first, and would allow for a smaller equivalent system. In contrast, to determine the impact of the GICs on the second requires power flow studies as described in [11], [12], and [13]. The set of transformers for which the reactive power losses need to be calculated [i.e., using (10)] has not been addressed in this paper. Such transformers would need to be included in an equivalent. This is an area for future study, undoubtedly building upon the rich voltage stability literature.

References

[1] V. D. Albertson, J. M. Thorson, Jr., R. E. Clayton, and S. C. Tripathy, "Solar-induced-currents in power systems: Cause and effects," *IEEE Trans. Power App. Syst.*, vol. PAS-92, no. 2, pp. 471–477, Mar./Apr. 1973.

[2] NERC, 2012 Special Reliability Assessment Interim Report: Effects of Geomagnetic Disturbances on the Bulk Power System, Feb. 2012.

[3] V. D. Albertson and J. A. Van Baelen, "Electric and magnetic fields at the earth's surface due to auroral currents," *IEEE Trans. Power App. Syst.*, vol. PAS-89, pp. 578–584, Apr. 1970.

[4] D. H. Boteler, "Geomagnetically induced currents: Present knowledge and future research," *IEEE Trans. Power Del.*, vol. 9, pp. 50–58, Jan. 1994.

[5] K. Zheng, R. J. Pirjola, D. H. Boteler, and L. Liu, "Geoelectric fields due to small-scale and large-scale currents," *IEEE Trans. Power Del.*, vol. 28, pp. 442–449, Jan. 2013.

[6] J. L. Gilbert, "Modeling the effect of the ocean-land interface on induced electric fields during geomagnetic storms," *Space Weather*, vol. 3, pp. 1–9, 2005.

[7] R. Pirjola, "Practical model applicable to investigating the coast effect of the geoelectric field in connection with studies of geomagnetically induced currents," *Adv. Appl. Phys.*, vol. 1, no. 1, pp. 9–28, 2013.

[8] R. J. Pirjola, "On the flow of geomagnetically induced currents in an electric power transmission network," *Canadian J. Phys.*, vol. 88, no. 5, pp. 357–363, May 2010.

[9] R. Pirjola and M. Lehtinen, "Currents produced in the Finnish 400 kV power transmission grid and the Finnish natural gas pipeline by geomagnetically-induced electric fields," *Ann. Geophys.*, vol. 3, no. 4, pp. 485–491, Apr. 1985.

[10] *Environmental and Space Electromagnetics*, H. Kikuchi, Ed. Hong Kong: Springer-Verlag, 1991, vol. , ch. 6.4 (edited by R. Pirjola and A. T. Viljanen), pp. 276–287.

[11] V. D. Albertson, J. G. Kappenman, N. Mohan, and G. A. Skarbakka, "Load-flow studies in the presence of geomagnetically-induced currents," *IEEE Trans. Power App. Syst.*, vol. PAS-100, pp. 594–606, Feb. 1981.

[12] J. Kappenman, Geomagnetic Storms and Their Impacts on the U.S. Power Grid, Metatech Corporation Report Meta-R-319, Jan. 2010.

[13] T. J. Overbye, T. R. Hutchins, K. Shetye, J. Weber, and S. Dahman, "Integration of geomagnetic disturbance modeling into the power flow: A methodology for large-scale system studies," in *Proc. 2012 North American Power Symp.*, Champaign, IL, USA, Sep. 2012.

[14] E. E. Bernabeu, "Modeling geomagnetically induced currents in Dominion Virginia power using extreme 100-year geoelectric field scenarios-part 1," *IEEE Trans. Power Del.*, vol. 28, pp. 516–523, Jan. 2013.

[15] D. H. Boteler and R. J. Pirjola, "Modeling geomagnetically induced currents produced by realistic and uniform electric fields," *IEEE Trans. Power Del.*, vol. 13, pp. 1303–1308, Oct. 1998.

[16] R. Horton, D. H. Boteler, T. J. Overbye, R. J. Pirjola, and R. Dugan, "A test case for the calculation of geomagnetically induced currents," *IEEE Trans. Power Del.*, vol. 27, pp. 2368–2373, Oct. 2012.

[17] X. Dong, Y. Liu, and J. G. Kappenman, "Comparative analysis of exciting current harmonics and reactive power consumption from GIC saturated transformers," in *Proc. IEEE PES 2001 Winter Meeting*, Columbus, OH, USA, Jan. 2001, pp. 318–322.

[18] K. Zheng, D. H. Boteler, R. Pirjola, L. G. Liu, R. Becker, L. Marti, S. Boutilier, and S. Guillon, "Influence of system characteristics on the amplitudes of geomagnetically induced currents," unpublished.

[19] R. A. Walling and A. H. Khan, "Characteristics of transformer exciting current during geomagnetic disturbances," *IEEE Trans. Power Del.*, vol. 6, pp. 1707–1713, Oct. 1991.

[20] O. Alsac, J. Bright, M. Prais, and B. Stott, "Further developments in LP-based optimal power flow," *IEEE Trans. Power Syst.*, vol. 5, pp. 697–711, Aug. 1990.

[21] W. F. Tinney, V. Brandwajn, and S. M. Chan, "Sparse vector methods," *IEEE Trans. Power App. Syst.*, vol. PAS-104, pp. 295–301, Aug. 1985.

[22] D. H. Boteler, Q'. Bui-Van, and J. Lemary, "Directional sensitivity of geomagnetically induced currents of the Hydro-Quebec 735 kV power system," *IEEE Trans. Power Del.*, vol. 9, pp. 1963–1971, Oct. 1994.

[23] K. Zheng, L. G. Liu, H. Y. Ge, and W. X. Li, "Comparative study of the GIC amplitudes and characteristics in different power grids in China," in *Proc. 44th CIGRE*, Paris, France, Aug. 2012.

[24] K. S. Shetye, T. J. Overbye, Q. Qiu, and J. A. Fleeman, "Geomagnetic disturbance modeling results for the AEP system: A case study," in *Proc. IEEE PES 2013 General Meeting*, Vancouver, BC, Canada, Jul. 2013, accepted for publication.

[25] S. Deckmann, A. Pizzolante, A. Monticelli, B. Stott, and O. Alsac, "Studies on power system load flow equivalencing," *IEEE Trans. Power App. Syst.*, vol. PAS-99, pp. 2301–2310, Nov./Dec. 1980.

Thomas J. Overbye (S'87–M'92–SM'96–F'05) was born in Milwaukee, WI, USA. He received the B.S., M.S., and Ph.D. degrees in electrical engineering from the University of Wisconsin, Madison, WI, USA.

He was with Madison Gas and Electric Company, Madison, WI, USA, from 1983 to 1991. He is currently the Fox Family Professor of Electrical and Computer Engineering at the University of Illinois, Urbana-Champaign, IL, USA. His current research interests include power system visualization, power system dynamics, power system cyber security, and power system geomagnetic disturbance analysis.

Komal S. Shetye (S'10–M'11) was born in Mumbai, India. She received the B.Tech. (2009) and M.S. (2011) degrees, both in electrical engineering, from the University of Mumbai, and the University of Illinois at Urbana-Champaign, USA, respectively.

She was a Graduate Research Assistant at the University of Illinois, from 2009 to 2011. She is currently a Research (Power) Engineer at the Information Trust Institute. Her current research interests include power system dynamics and stability, and power system geomagnetic disturbance analysis.

Trevor R. Hutchins (S'10) was born in Amarillo, TX, USA. He received the B.S. (2009) and M.S. (2012) degrees, both in electrical and computer engineering, from Baylor University and the University of Illinois at Urbana-Champaign, USA, respectively.

His current research interests include the impact of high impact low frequency events on power systems.

Qun Qiu (SM'12) received the master degree in computer engineering and the Ph.D. degree in electrical engineering from Virginia Tech, Blacksburg, VA, USA.

He is Principal Engineer at American Electric Power, responsible for AEP and collaborative R&D projects, and industry-wide investigations aligned with business purposes. He joined AEP in 2002. He serves as a member of the North American Electric Reliability Corporation (NERC) Geomagnetic Disturbances Task Force, an advisor of Electric Power Research Institute Transmission & Substation Area Task Force, etc.

Dr. Qiu is a registered Professional Engineer in the State of Ohio.

James D. Weber (S'92–M'99) was born in Platteville, WI, USA. He received the B.S. degree in electrical engineering from the University of Wisconsin-Platteville in 1995 and the M.S. and Ph.D. degrees in electrical engineering from the University of Illinois at Urbana-Champaign, USA, in 1997 and 1999.

He worked at Wisconsin Power and Light (now part of American Transmission Company) in the summer of 1994 and 1995. He is the Director of Software Development at PowerWorld Corporation in Champaign, IL, USA, a position he has held since 1999, where he oversees the staff working on all of PowerWorld's software tools.